US007564162B2

(12) **United States Patent**
Ho et al.

(10) **Patent No.: US 7,564,162 B2**
(45) **Date of Patent: Jul. 21, 2009**

(54) **PROCESS COMPENSATED MICROMECHANICAL RESONATORS**

(75) Inventors: **Gavin Kar-Fai Ho**, Cambridge, MA (US); **Farrokh Ayazi**, Atlanta, GA (US)

(73) Assignee: **Georgia Tech Research Corp.**, Atlanta, GA (US)

(*) Notice: Subject to any disclaimer, the term of this patent is extended or adjusted under 35 U.S.C. 154(b) by 37 days.

(21) Appl. No.: **12/001,341**

(22) Filed: **Dec. 11, 2007**

(65) **Prior Publication Data**

US 2008/0143217 A1 Jun. 19, 2008

Related U.S. Application Data

(60) Provisional application No. 60/869,821, filed on Dec. 13, 2006.

(51) **Int. Cl.**
H02N 2/00 (2006.01)

(52) **U.S. Cl.** **310/309**; 333/186

(58) **Field of Classification Search** 310/309; 333/186, 188, 200; 73/504.03, 504.12, 504.14, 73/514.32, 514.37, 514, 38, 862.59
See application file for complete search history.

(56) **References Cited**

U.S. PATENT DOCUMENTS

5,396,066 A * 3/1995 Ikeda et al. 250/306
2006/0125576 A1 * 6/2006 Ho et al. 333/186

* cited by examiner

Primary Examiner—Thomas M Dougherty
(74) *Attorney, Agent, or Firm*—Kenneth W. Float

(57) **ABSTRACT**

Disclosed are micromechanical tapered I-shaped bulk acoustic resonators. An exemplary resonator is formed on a substrate, which is preferably silicon. The resonator has a central rod (or extensional member) coupled to two tapered lateral flanges (or flexural members). The central extensional member and tapered flexural members are separated from the substrate. One or more electrodes are disposed adjacent to the tapered flexural members, are separated therefrom by small gaps, and are separated from the substrate. One or more anchors are coupled to the substrate, are laterally separated from the central rod by small gaps, and are coupled to the central rod by supports. The one or more anchors support and suspend the central rod and flexural members from the substrate. Process compensation is achieved using the tapered flexural members.

4 Claims, 5 Drawing Sheets

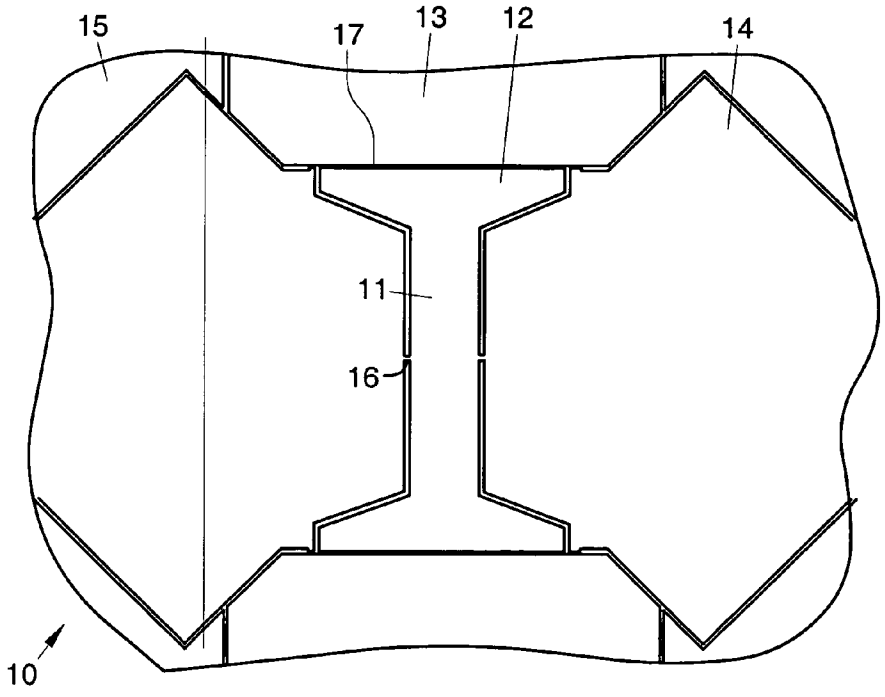

Fig. 1

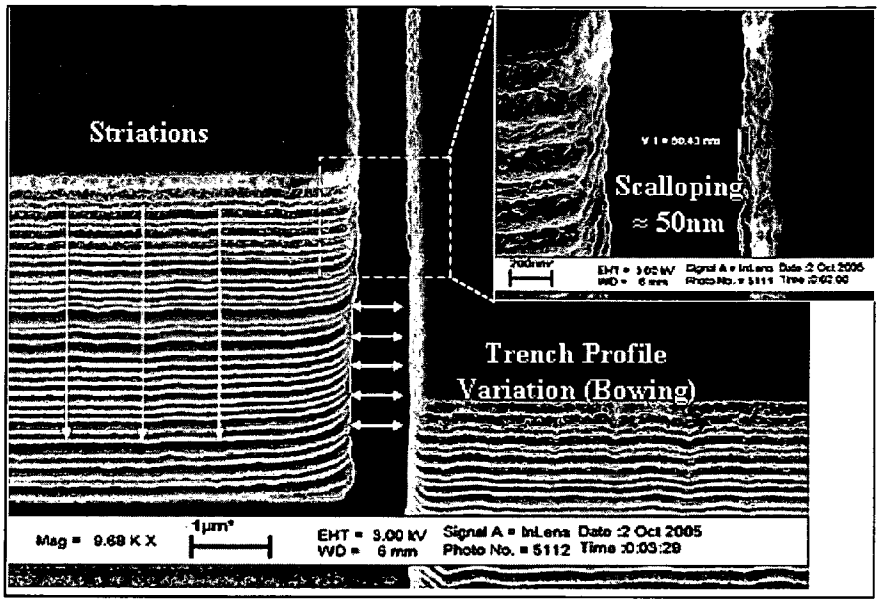
Striations
Scalloping
≈ 50nm
Trench Profile
Variation (Bowing)
Mag = 9.69 K X
1µm
EHT = 3.00 kV
WD = 6 mm
Signal A = InLens Date :2 Oct 2005
Photo No. = 5112 Time :0:03:29

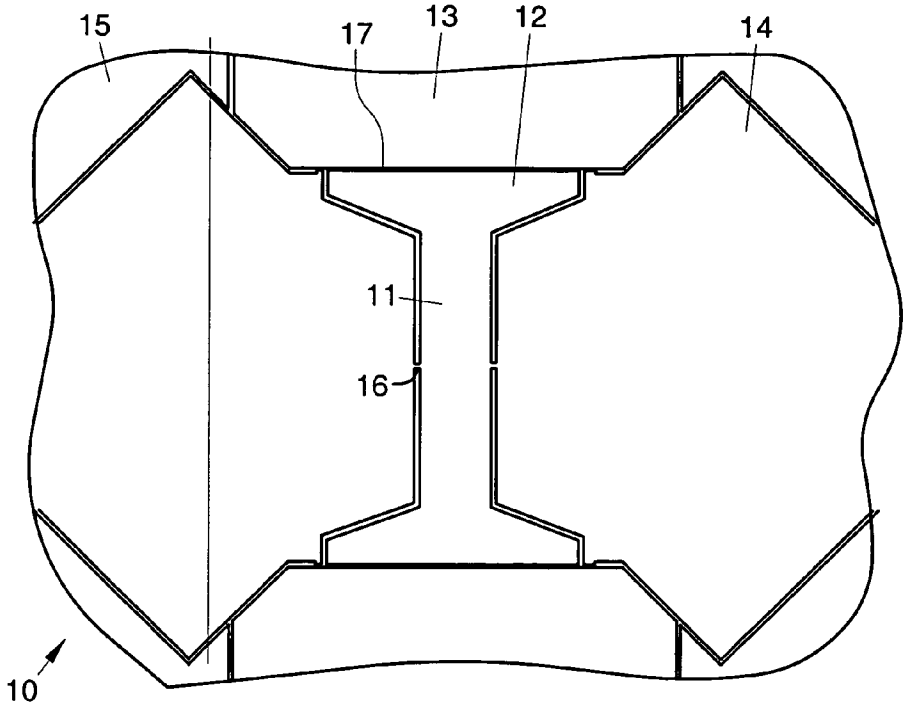
15
17
13
12
14
11
16
10

Fig. 2

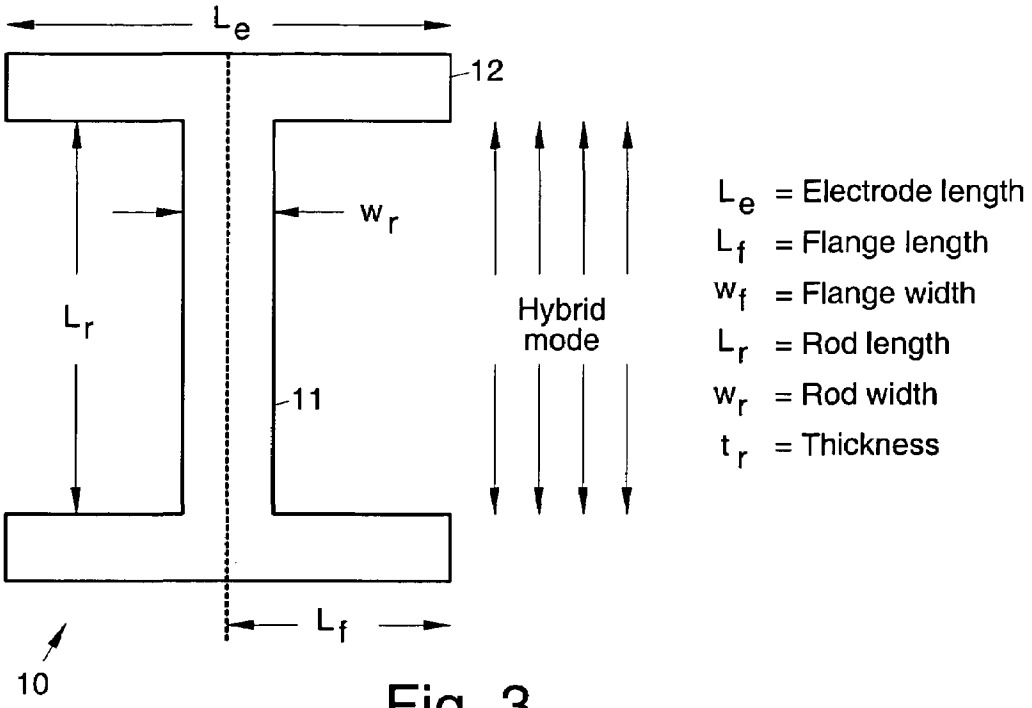

Fig. 3

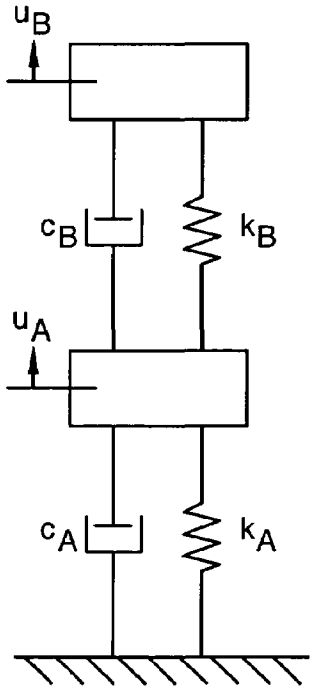

Fig. 4a

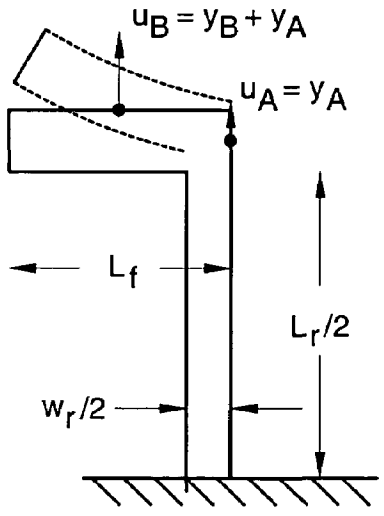

Fig. 4b

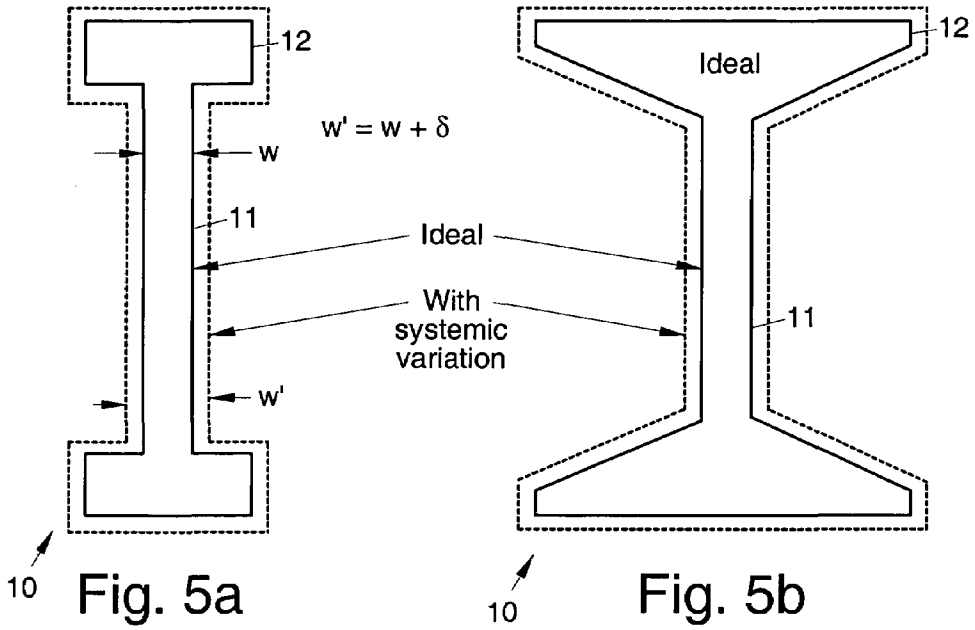

Fig. 5a Fig. 5b

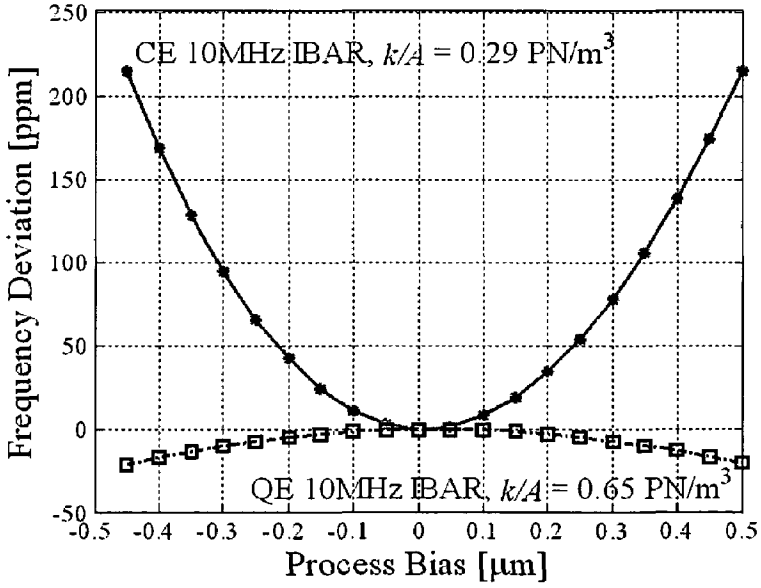

Fig. 6

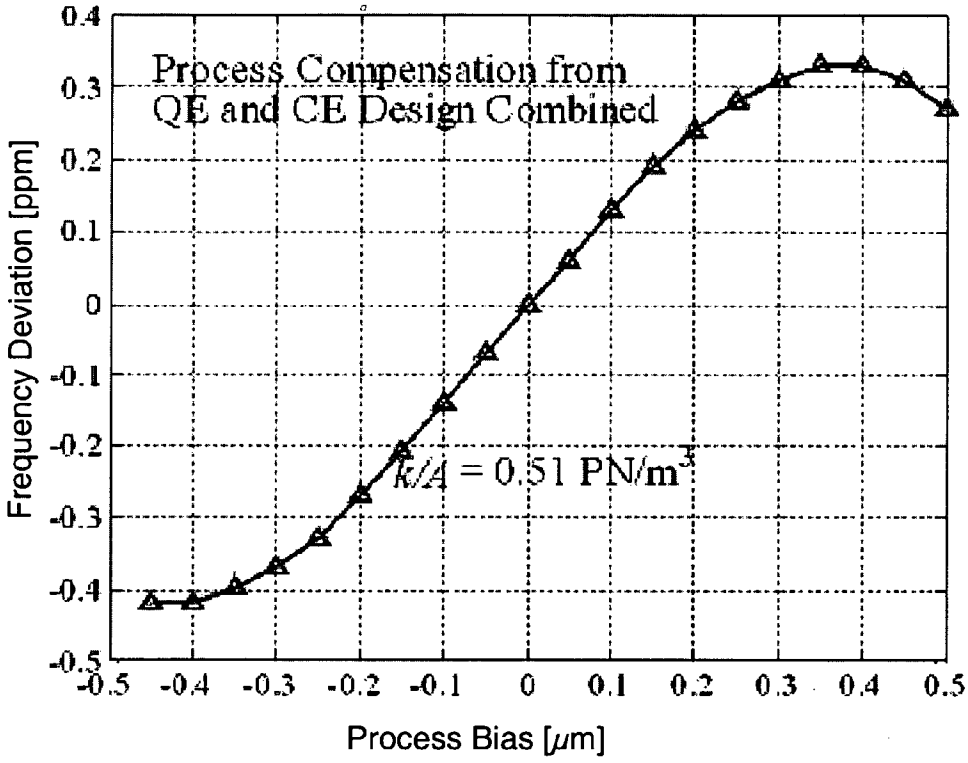
Process Compensation from
QE and CE Design Combined
$k/A = 0.51$ PN/m^3
Frequency Deviation [ppm]
Process Bias [μm]
0.4
0.3
0.2
0.1
0
-0.1
-0.2
-0.3
-0.4
-0.5
-0.5 -0.4 -0.3 -0.2 -0.1 0 0.1 0.2 0.3 0.4 0.5

Fig. 7

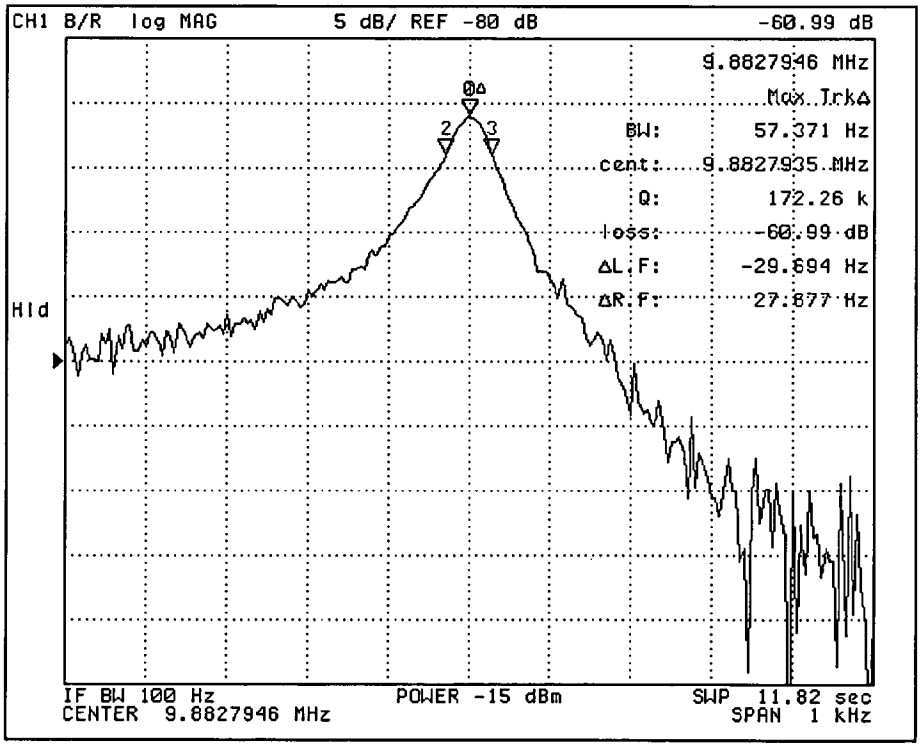
CH1 B/R log MAG
5 dB/ REF -80 dB
-60.99 dB
9.8827946 MHz
Mkr Trk
BW: 57.371 Hz
cent: 9.8827935 MHz
Q: 172.26 k
loss: -60.99 dB
ΔL.F: -29.694 Hz
ΔR.F: 27.877 Hz
Hld
IF BW 100 Hz
CENTER 9.8827946 MHz
POWER -15 dBm
SWP 11.82 sec
SPAN 1 kHz

Fig. 8

Fig. 9

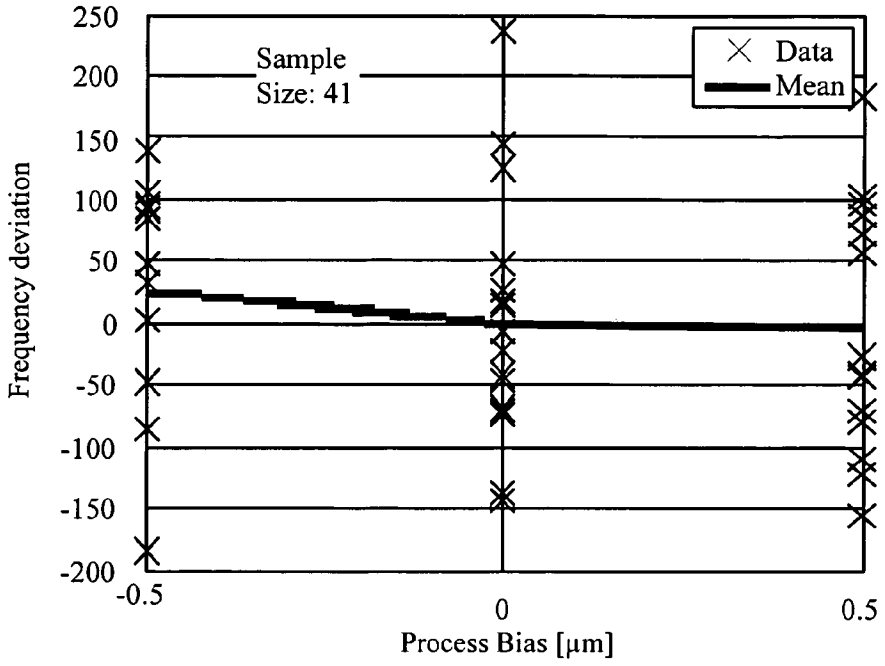

Fig. 10

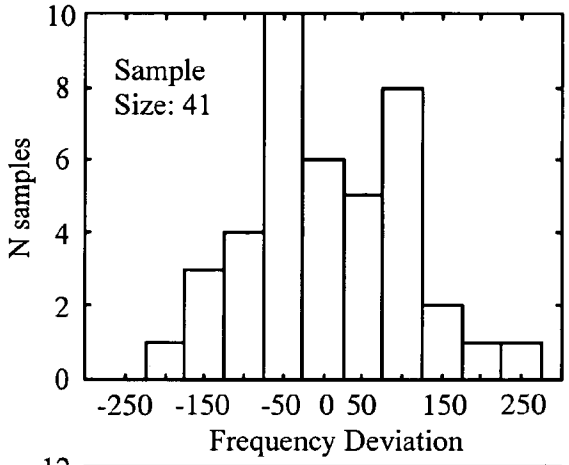

Fig. 11

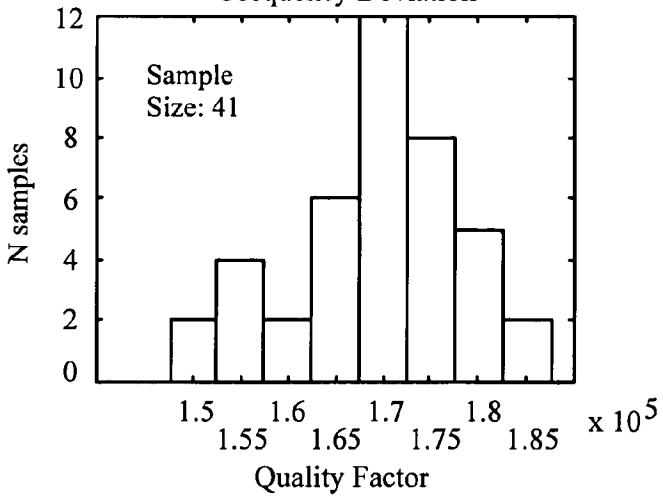

PROCESS COMPENSATED MICROMECHANICAL RESONATORS

This application claims the benefit of U.S. Provisional Application No. 60/869,821, filed Dec. 13, 2006.

BACKGROUND

The present invention relates to micromechanical I-shaped bulk acoustic resonators (IBARs).

Micromechanical resonators are strong candidates to complement quartz technology in frequency references. Frequency accuracy is a key technological hurdle that must be addressed. Deviations in center frequency can be attributed to material properties and geometry. To address this issue, center frequency trimming by iterative laser ablation and by selective deposition have been proposed. Individually-programmed synthesizers utilizing fractional-N phase lock loops (PLLs) have also been demonstrated. However, a design for manufacturability (DRM) technique employing batch compensation would address the issue at its roots.

The material properties must be consistent and repeatable to enable DFM. Single-crystal silicon (SCS) is the choice material since it is the best controlled and most characterized. Its ideal crystalline nature also has potential for very high Q and minimal aging. For reference, quartz crystal units typically have absolute frequency tolerances up to ±20 ppm. Hence, the applicability of micromechanical resonators is contingent on meeting similar performance metrics.

It would be desirable to have improved micromechanical resonators and fabrication methods. In particular, it would be desirable to have improved micromechanical tapered I-shaped bulk acoustic resonators.

BRIEF DESCRIPTION OF THE DRAWINGS

The various features and advantages of the present invention may be more readily understood with reference to the following detailed description taken in conjunction with the accompanying drawings, wherein like reference numerals designate like structural elements, and in which:

FIG. **1** illustrates a SEM view of a typical 10 μm DRIE trench in a SOI substrate;

FIG. **2** illustrates a SEM view of an exemplary DFM-optimized 10 MHz IBAR;

FIG. **3** illustrates the geometry of an exemplary IBAR;

FIG. **4** illustrates a lumped 2DOF ¼-model of an exemplary IBAR;

FIGS. **5***a* and *b* illustrates dimensional dependency on trench width for a QE IBAR and a CE IBAR, respectively;

FIG. **6** is a graph that illustrates simulated f_n variation of 10 MHz QE and CE IBARs for δ=[−0.5,0.5]μm;

FIG. **7** is a graph that illustrates the natural frequency dependency of a 10 MHz optimized IBAR on process bias δ;

FIG. **8** is a graph that illustrates typical frequency response from the optimized 10 MHz IBAR with V_P=25V and P=5 Torr;

FIG. **9** is a graph showing measured frequency deviation from the ideal design and designs with deliberately drawn bias;

FIG. **10** shows a histogram of resonator frequencies; and

FIG. **11** shows a histogram of resonator Q.

DETAILED DESCRIPTION

Referring to the drawing figures, disclosed are process compensated micromechanical resonators **10**, whose center frequency is robust to dimensional variations caused by lithography and micromachining. Exemplary embodiments of the process compensated micromechanical resonators **10** comprise tapered I-shaped bulk acoustic resonators **10**.

The exemplary resonators **10** described herein may be fabricated using fabrication processes described in U.S. application Ser. No. 11/251,197, filed Oct. 15, 2005, for example, the contents of which are incorporated herein by reference in their entirety.

In developing the improved resonators **10**, non-idealities of silicon bulk micromachining of a typical conventional resonator shown in FIG. **1** are analyzed along with their effects on resonator characteristics. FIG. **3** shows the geometry of an exemplary I-shaped bulk acoustic resonator (IBAR). A very simple lumped model of an IBAR is disclosed with reference to FIGS. **4***a* and **4***b*. Process compensation techniques for exemplary IBARs are discussed and validated using finite element simulations. Experiments and verification of the process compensation scheme are discussed.

Silicon Micromachining and Process Compensation

High performance capacitive resonators must have a large transduction area. This requirement calls for deep reactive ion etching (DRIE) of thick resonators whether trenches are used for transduction or are used to define sacrificial gaps. In trench etching, non-idealities such as scalloping, striations, bowing, and footing exist, as is illustrated in FIG. **1**. The first three phenomena are generally random and are typically within 50 nm. In optimized processes, footing can be avoided and random non-idealities are further reduced.

Lithography and pattern transfer issues account for the majority of micromachining variations. These limit the dimensional accuracy which generally compromises center frequency accuracy. Although these variations are temporally random, they are spatially systematic.

Process compensation with regard to the center frequency is conceptually straightforward. Since critical dimension (CD) variations lead to deviations from the modal stiffness k and mass m, the process-compensated design ensures that variations in k are proportional to variations in m, thus maintaining a constant f_n, given by

$$f_n = \tfrac{1}{2}\pi\sqrt{k/m}. \quad (1)$$

Resonator Design and Modeling

A simple lumped mechanical model of the IBAR **10** is discussed below. Three categories of IBARs **10**, including Q-enhanced (QE), compliance-enhanced (CE), and semi-compliant high-Q (CQ) IBARs **10**, are discussed and contrasted. A 10 MHz optimized semi-compliant high-Q IBAR **10** is detailed and its frequency-sensitivity is modeled.

FIG. **2** illustrates an exemplary IBAR **10**. The IBAR **10** is formed on a substrate **15**, which is preferably a silicon substrate **15**. The IBAR **10** has a central rod **11** (or extensional member **11**) coupled to two tapered lateral flanges **12** (or flexural members **12**). The central extensional member **11** and tapered flexural members **12** are separated (released) from the substrate **15**. One or more electrodes **13** are disposed adjacent to the tapered flexural members **12**, are separated therefrom by small gaps **17**, and are separated (released) from the substrate **15**. One or more anchors **14** are coupled to the substrate **15**, and are coupled to the central rod **11** by supports **16**. The one or more anchors **14** function to support and suspend the central rod **11** and flexural members **12** from the substrate **15**. The supports **16** are placed in such a way to minimize acoustic loss to the substrate **15** and enable maximum Q. The extensional member **11**, the tapered flexural members **12**, the anchors **14**, and the supports **16** are preferably made of low-resistivity single crystal silicon (SCS). The

electrodes **13** are preferably LPCVD trench-refilled doped polysilicon. Various parameters are shown in FIG. **3**, including electrode length, flange length, flange width, rod length rod width and thickness.

A preferred method of fabricating the resonator **10** begins with a singly crystal silicon (SCS) layer on an insulating oxide layer on a substrate **15**, otherwise known as a silicon-on-insulator (SOI) substrate **15**. Trenches are etched in the SCS layer to define the tapered lateral flanges **12** (tapered flexural members **12**), the rod **11** (or extensional member **11**), and the supports **16**. A thin sacrificial oxide layer is then grown or deposited and the trenches are refilled with polysilicon to form the electrodes **13**. The polysilicon is patterned to define pads for the electrodes **13**. Parts of the SCS layer are etched and the resonator **10**, anchors **14**, supports **16**, and silicon pads are defined. By etching the sacrificial oxide and insulating layer, the resonator **10** becomes released with gap **17** formed between the tapered lateral flanges **12** and the electrodes **13** and is suspended above the substrate **15**.

A simple two degree-of-freedom system is shown in FIGS. **4***a* and **4***b* that may be used to analyze the IBAR **10**. The model includes an extensional component (rod **11**) and a flexural component (flanges **12**). Damping in the model is assumed to be intrinsic (i.e., by material losses and not air damping or anchor loss) and proportional to velocity. The coupled two degree-of-freedom system includes lumped parameters m_i, k_i, and c_i for I=A, B, which are derived from parameters of constituent components. Local coordinates y_i model local displacements of each component and u_i represent global displacements.

The three categories of IBARs **10** may be described using FIGS. **4***a* and **4***b*. The eigenvalue problem describing the 2 degree-of-freedom system yields eigenvectors (i.e., mode shapes) that are dependent on the lumped parameters. The system can have two modes. The mode of interest is the lower frequency mode in which mass elements are in phase. For the sake of brevity, the three classifications are described without mathematical detail.

For the case in which k_B is very large, the mode is predominantly in extension of the rod (i.e. $y_B<<y_A$). The mass m_B can be viewed as a mass-loading energy storage element. If losses in the system are entirely intrinsic, increasing m_B actually increases the quality factor. IBARs **10** with this characteristic are the Q-enhanced (QE) class. Although Q is greater than a uniform extensional rod, the f·Q product remains constant.

At the other extreme, k_B is small and y_B is dominant. For this case, the stiffness, Q, and natural frequency of the IBAR **10** are solely defined by the flexural flange **12**. These are compliance-enhanced (CE) IBARs **10** since the stiffness is low in comparison to a purely extensional mode. Compliance enhancement leads to reduced motional impedance and high electrostatic tuning.

The semi-compliant high-Q (CQ) IBAR **10** combines the attractive features of both extreme topologies. These structures have reduced stiffness and enhanced Q. It will be shown that the semi-compliant high-Q (CQ) IBAR **10** is also ideal for DFM.

Q-Enhanced (QE) IBAR DFM

The geometry of a Q-enhanced (QE) IBAR and the dependence of its geometry on systematic process variations is shown in FIG. **5***a*. Process bias δ due to DR_rIE trench width variation affects all features equally. For a process-compensated design, the gradient of natural frequency on process bias is ideally zero. Using the crude two degree-of-freedom model, the natural frequency of a Q-enhanced (QE) IBAR **10** is $\mathrm{sqrt}(k_A/(m_A+m_B))$. For $w=w_f$ the zero-frequency-sensitivity problem is solved for $L_r/L_f=4$. A ratio of 4 is a typical lower limit. If flexing or shearing is considered in the model, the ratio is greater. Thus, the half-length of the electrode is less than ¼ of the length of the rod **11**.

The result may be verified using finite element analysis. The geometry for a 10 MHz resonator was obtained using the mechanical properties of single crystal silicon. The L_f/L_r ratio is 6.1. As is shown in FIG. **6**, frequency variations due to ±0.5 μm process bias were simulated to be [−25, 0]ppm.

Compliance-Enhanced (CE) IBAR DFM

A compliance-enhanced (CE) IBAR has greatest contribution from the flexural component (flanges). Therefore, to compensate for processing variations in a compliance-enhanced (CE) IBAR, the flexural component (flanges) must be compensated. It can be shown that a tapered clamped-free beam (rod) can be process compensated.

A process compensated 10 MHz compliance-enhanced (CE) IBAR **10** incorporating tapered flanges **12** for compensation is shown in FIG. **5***b*. The variation in its natural frequency is 220 ppm for a process bias of ±−0.5 μm and the curvature of the frequency sensitivity is positive, as shown in FIG. **6**. When compared to the 10 MHz Q-enhanced (QE) IBAR **10**, the absolute frequency variation is increased because the tip of the tapered flange **12** is relatively small.

Optimized 10 MHz Semi-compliant High-Q (CQ) IBAR DFM

In the design of the Q-enhanced (QE) IBAR **10**, normalized stiffness is high and therefore motional resistance is high and tuning is reduced. In the design of the compliance-enhanced (CE) IBAR, the area and compliance are much greater, but a small feature is required for compensation. To optimize, both compensation techniques are used in a semi-compliant high-Q (CQ) IBAR **10** which has both extensional and tapered flexural contributions to the mode shape.

This methodology was used to fabricate a 10 MHz 10 μm thick semi-compliant high-Q (CQ) IBAR **10** shown in FIG. **2**. Tapering in the flange **12** is reduced and partial extension of the rod **11** is present in the mode. Thus, both forms of compensation are in effect. The variation in f_n is ±0.4 ppm over a processing window of ±0.5 μm, as shown in FIG. **7**.

A disk or extensional resonator is an excellent basis for comparison since its dimensions are the largest for a given frequency. Since the natural frequency of an extensional resonator is $f_n=nv_a(2L)^{-1}$, the frequency-sensitivity is

$$\frac{df/f_n}{dL} = -\frac{2f_n}{nv_a}, \tag{2}$$

where the acoustic velocity v_a is ~8500 m/s along <110>. A fundamental extensional mode resonator at 10 MHz will have a frequency variation of 2400 ppm for dL=1 μm. Therefore, Q-enhanced (QE) and semi-compliant high-Q (CQ) IBARs **10** are at least a factor of 100 less sensitive to process bias. The frequency dependence on thickness if the IBAR **10** was also simulated using finite element analysis. For a thickness variation of ±1 μm, the f_n variation is ~46 ppm.

Experimentation

To verify the optimized design, dimensional variations due to process bias was replicated using e-beam lithography. Three designs were drawn: a nominal 10 MHz semi-compliant high-Q (CQ) IBAR **10** with ideal geometry, one with −0.5 μm bias, and one with +0.5 μm bias. Devices were fabricated on a 10 μm n-type 0.002 Ω-cm SOI substrate **15**, as shown in FIG. **2**. 400 nm capacitive gaps **17**, **18** were dry etched in a Surface Technology Systems Limited etching tool, and

released in 49% HF solution. No steps were taken to reduce roughness. This described process is another embodiment to form resonator **10**.

The experimental setup included an Agilent 4395A network analyzer and a vacuum chamber. The typical frequency response from an IBAR **10** is shown in FIG. **8** had an impressive quality factor of 170000 in low vacuum (5 Torr). Some resonators **10** were tested in high vacuum, at which the quality factors exceeded 250000. A polarization voltage of 25V was applied to all resonators **10**.

The measured frequency variation across 41 resonators **10** was within ±250 ppm as shown in FIG. **9**. The frequency variations are dispersed. However, less than 25 ppm variation was observed in the mean frequencies of the three designs. Thus, the ±250 ppm variation can be attributed to random variations.

Histograms of center frequency and Q are shown in FIGS. **10** and **11**, respectively. The mean frequency from the 41 samples is 9.884 MHz. Inaccuracies in the material properties are the cause of the 1.2% frequency error. In practice, characterized substrates and precision tools to align to crystal axes are available. The elasticity coefficients and mass density are doping-dependant and are generally known within a few hundred ppm. Oxidation or hydrogen annealing of the IBARs **10** reduces random frequency variations and yields measurement accuracy of ~10 ppm and theoretical limits. Data from resonators **10** having a Q lower than 130000 were discarded due to cleanliness since particles on the surfaces also load the frequency. Measurement data from all other resonators are reported.

Process Compensation of CE IBARs

As discussed above, a IBAR is a coupled resonator having an extensional member and at least one flexural member that can be modeled as a two degree-of-freedom system. It was demonstrated through simulation that an IBAR can be processed compensated. However, the previous geometry was not compliance-enhanced (i.e., not tunable).

For the compliance-enhanced IBAR **10**, the modal displacement y_B of the flexural component **12** is significantly greater than the modal displacement y_A of the extensional part. According to Dunkerley's formula,

$$\frac{1}{\omega^2} = \sum_i \frac{1}{\omega_i^2} \tag{3}$$

in which ω is the resonance frequency of the combined system, and ω_i are the resonance frequencies of the individual components, the resonance frequency of the flexural component **12** predominantly defined the fundamental resonance frequency of the compliance-enhanced IBAR **10**. Thus, in order to process compensate a compliance-enhanced IBAR **10**, process compensation must be enabled in the flexural component **12** (or beam).

Uniform beams, in which the cross-section is constant along the length, cannot be process compensated. Without going into mathematical detail, a tapered beam (flexural component **12**) can be process compensated.

With this established, compliance-enhanced IBARs **10** can be process compensated.

The above-disclosed design for manufacturability (DFM) technique for mechanical process compensation enables fabrication of IBARs **10** with repeatable intra- and inter-run frequencies. The disclosed approach defines process bias (CD variation) windows for silicon micromachining to obtain a center frequency within acceptable tolerances. Resonators **10** with features for process compensation have been disclosed that may be used as low-power temperature-stable frequency references. Repeatable high quality factors and resonator frequencies have been demonstrated.

Thus, improved micromechanical tapered I-shaped bulk acoustic resonators have been disclosed. It is to be understood that the above-described embodiments are merely illustrative of some of the many specific embodiments that represent applications of the principles discussed above. Clearly, numerous and other arrangements can be readily devised by those skilled in the art without departing from the scope of the invention.

What is claimed is:

1. Micromechanical resonator apparatus, comprising:

a substrate; and

resonator apparatus comprising:

one or more anchors connected to the substrate;

at least one input/output electrode that is electrically insulated from the substrate; and

a resonator comprising an extensional member coupled to the anchor and separated from the substrate, and a plurality of tapered flexural members connected to the extensional member that are separated from the substrate and separated from the electrode by capacitive gaps.

2. The apparatus recited in claim **1** wherein the plurality of tapered flexural members are separated from the at least one input/output electrode by a gap.

3. The apparatus recited in claim **1** wherein width and length dimensions of the tapered flexural member and the extensional member are controlled so that the stiffness-to-mass ratio of the resonator is substantially independent of processing variations.

4. The apparatus recited in claim **1** wherein the resonator apparatus further comprises:

at least one additional input/output electrode that is electrically insulated from the substrate, and is disposed on an opposite side of the flexural member from the at least one electrode, and is separated from the at least one tapered flexural member by a gap.

* * * * *